Skeleton Isomerization of Dithiophenebenzo-4,5-Dione Enabling Efficient n-Type Cathode Material for Sodium-Ion Batteries

Shunqi He[a], Lingxiao Gan[a], Xixi Cheng[a], Cheng Zhong[b, *], Fei Wu[a, *], Linna Zhu[a, *]

[a]*Chongqing Key Laboratory for Advanced Materials and Technologies of Clean Energy, School of Materials & Energy, Southwest University, Chongqing 400715, P. R. China.*

[b]*Hubei Key Lab on Organic and Polymeric Optoelectronic Materials, Department of Chemistry and Molecular Science, Wuhan University, Wuhan 430072, P. R. China*

E-mail address: lnzhu@swu.edu.cn (L. Zhu); feiwu610@swu.edu.cn (F. Wu)

Experimental Section

Materials： Unless otherwise stated, all raw materials can be used without further purification. 1,4-benzenediboronic acid bis(pinacol)ester (BDE), Benzo[1,2-b:6,5-b']Dithiophene-4,5-Dione, 3,3-Bithiophene, Oxalyl Chloride, ethanol, and 1,4-dioxane were purchased from Shanghai Titan Technology Co., Ltd.. Acetone was purchased from Chongqing Chuandong Chemical (Group) Co., Ltd. Ketjen Black and carboxymethylcellulose (CMC) were purchased from Guangdong candlelight new energy technology co., ltd. 1 M $NaPF_6$ in dimethoxyethane (DME) was purchased from Suzhou Duoduo Chemical Technology Co., Ltd..

Synthesis of PBD-1

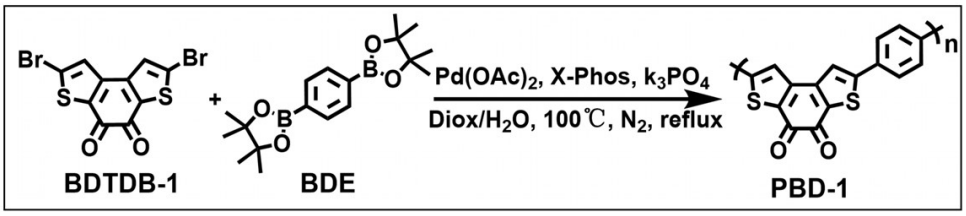

Scheme 1. Synthesis route and chemical structure of PBD-1.

A Schlenk tube was added with 2,7-dibromobenzo[1,2-b:4,3-b'] dithiophene-4,5-dione (BDTDB-1, 500 mg, 1.32 mmol), 1,4-benzenediboronic acid bis(pinacol)ester (BDE, 436 mg, 1.32 mmol), potassium phosphate (K_3PO_4, 1.68 g, 7.92 mmol), palladium acetate [$Pd(OAc)_2$, 17.8 mg], 2-(dicyclohexylphosphino)-2',4', 6'-triisopropylbiphenyl (X-Phos, 75.6 mg), 1,4-dioxane (27.5 ml) and deionized water (6.9 ml) under N_2 atmosphere. The mixture was firstly heated at 110°C for 3 days and then cooled to room temperature. 50 ml deionized water and 30 ml ethyl alcohol were added in the mixture and the precipitates were filtered. After drying at 100 °C for 24 h, the precipitates underwent Soxhlet extraction by using dichloromethane, tetrahydrofuran and ethyl acetate, respectively, for further purification. The PBD-1 was gained as a dark powder with a yield of 90%.

Synthesis of PBD-2

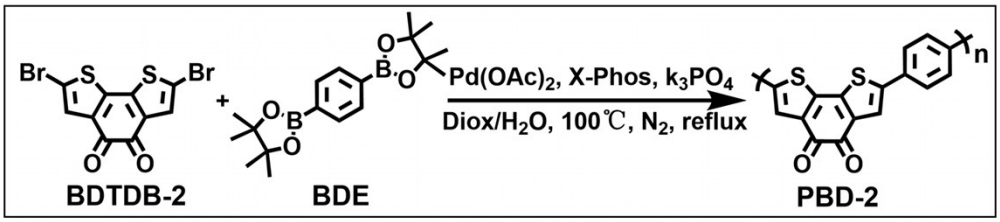

Scheme 2. Synthesis route and chemical structure of PBD-2.

The isomer PBD-2 was synthesized in a similar way. A Schlenk tube was added with 2,7-dibromobenzo[1,2-b:6,5-b']dithiophene-4,5-dione (BDTDB-2, 500 mg, 1.32 mmol), 1,4-benzenediboronic acid bis(pinacol)ester (BDE, 436 mg, 1.32 mmol), potassium phosphate (K_3PO_4, 1.68 g, 7.92 mmol), palladium acetate [$Pd(OAc)_2$, 17.8 mg], 2-(dicyclohexylphosphino)-2',4',6'-triisopropylbiphenyl(X-Phos, 75.6 mg), 1,4-dioxane (27.5 ml) and deionized water (6.9 ml) under N_2 atmosphere. The mixture was firstly heated at 110°C for 3 days and then cooled to room temperature. 50 ml deionized water and 30 ml ethyl alcohol were added in the mixture and the precipitates were filtered. After drying at 100 °C for 24 h, the precipitates underwent Soxhlet extraction by using dichloromethane, tetrahydrofuran and ethyl acetate, respectively, for further purification. The PBD-2 was a dark powder with a yield of 75%.

Characterizations

The Fourier transform infrared spectrometer (FT-IR) was recorded using KBr pellets on a Nicolet Nexus 670 with the wavenumber range of 400-4000 cm^{-1}. The morphology of the samples were measured by field-emission scanning electron microscope (FE-SEM, JEOL, JSM-7800F) and X-ray diffraction (XRD, SHIMADZU XRD-7000).The electrode sheets at different charging and discharging states were obtained by disassembling the battery in a glovebox filled with Ar (O_2 and H_2O content < 0.1 ppm), and then washed with DME to remove the residual electrolyte. Next, the electrodes were dried in vacuum for 2 hours, at 60 ℃. After that, the electrodes were marked and

stored in Ar-filled glove box. The samples were exposed in air during FTIR tests, and they were tested using the ATR pattern. For XPS tests, the samples were prepared in Ar atmosphere, and then the XPS measurements were carried out. UV-Vis absorption spectra were collected on LAMBDA 365+ UV/Vis Spectrometer.

Electrochemical measurements

CR 2032-coin cells were assembled in an argon filled glove box, to measure the electrochemical properties of the electrode materials.

For the half cell: The anode was sodium metal and the PBD-1/PBD-2 was fabricated from a slurry of 60 wt.% active material, 30 wt.% Ketjin black and 10 wt.% CMC as the binder. The loading mass of PBD-1/PBD-2 on Al foil were above 1.2 mg cm^{-2}. These slurries were blade cast onto aluminum current collector and dried at 60 ℃ for 8 hours before battery assembling. The cells were assembled with an electrolyte of 1 M $NaPF_6$ in dimethoxyethane (DME, 120 μl), a separator of Whatman glass fiber. The galvanostatic cycling test was carried on a CT-4008T instrument (Shen Zhen NEWARE electronic Co.) at 25 ℃. CVs were tested on a CHI instrument electrochemical work-station (CS 310m) at a scan rate of 2.0 mV s^{-1} between 1.0 and 3.0 V (vs. Na^+ /Na). The EIS test was measured by a CHI instrument electrochemical workstation in the frequency range of 0.01–10^5 Hz at the amplitude of 5 mV. The above tests were conducted at room temperature.

For the full-cell: The Bi-based half cells were cycled to prepare Na_3Bi alloy as the starting anode. The Bi-based anode electrodes were fabricated by 50 wt% Bi, 40 wt%

SP and 10 wt% CMC (binder). The slurry was casted on Cu foil (anode) then dried in oven at 60 ℃ for 8 hours. The neat loading mass of active material was above 1.2 mg cm^{-2} for all electrodes. Afterwards, the PBQ-1 electrodes and the Na_3Bi electrodes were used to construct the full cells, following the same procedures as half cells. The electrolyte was 1 M $NaPF_6$ in DME (120 μl). The separator was Whatman glass fiber.

Computational details

All optimizations were done at the PBE0/def2-SVP level with Grimme's D3BJ[1] empirical dispersion correction. All the calculations are performed using Gaussian 16 program.[2] The electrostatic potential calculation was performed using the Multiwfn program.

GITT test

The Na^+ diffusion coefficient (D_{Na^+}) was calculated by the galvanostatic intermittent titration technique measurement (GITT) method according to the following equation[3]:

$$D = \frac{4}{\pi\tau}\left(\frac{m_B V_M}{M_B S}\right)^2\left(\frac{\Delta E_s}{\Delta E_t}\right)^2 \quad (1)$$

where τ is the pulse time, V_m is the molar volume, S is the effective area of the electrodes (1.13 cm^2), ΔE_S is the voltage difference between the steady state and the initial state of every step, and ΔE_t is the change of total voltage during a pulse step

excluding the IR drop.

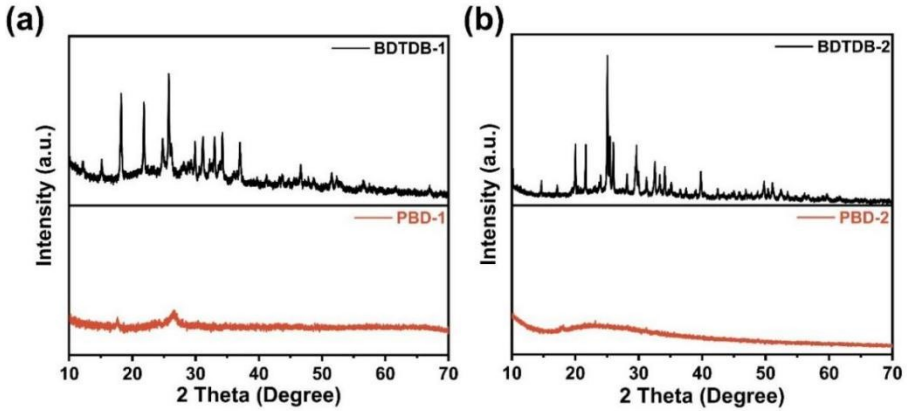

Figure S1. XRD spectra of PBD-1, PBD-2 and their monomers BDTDB-1 and BDTDB-2.

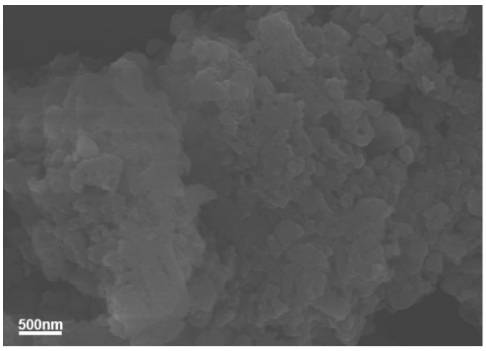

Figure S2. FE-SEM image of the PBD-1 powder.

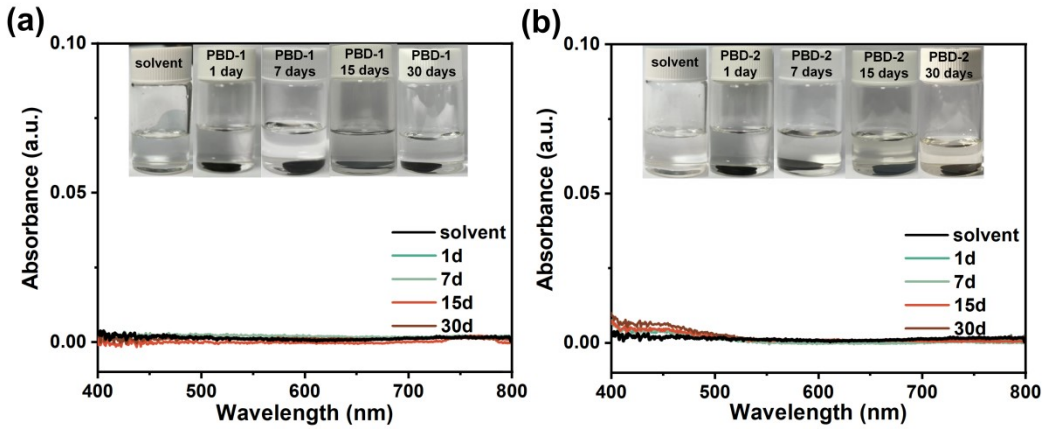

Figure S3. UV-vis spectra of solubility tests with (a) PBD-1 and (b) PBD-2 electrode sheets immersed in DME solvent.

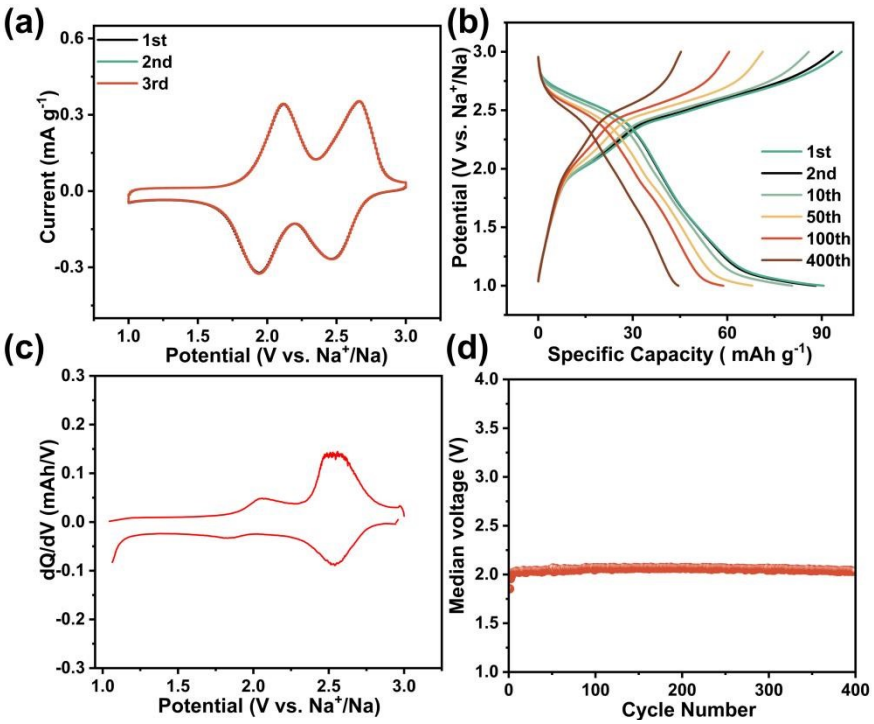

Figure S4. Electrochemical characterization of PBD-2: a) CV curves at 2 mV s^{-1}; b) Charge–discharge curves at 0.5C; c) dQ/dV curve at 0.5C; d) Median voltage curve at 0.5C.

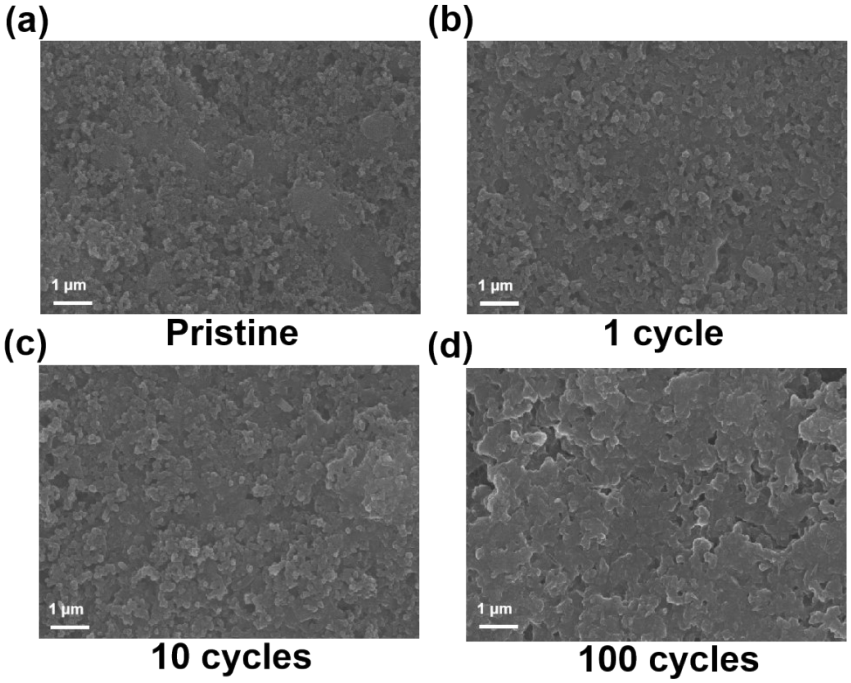

Figure S5. SEM images of the PBD-1 electrode at different cycles.

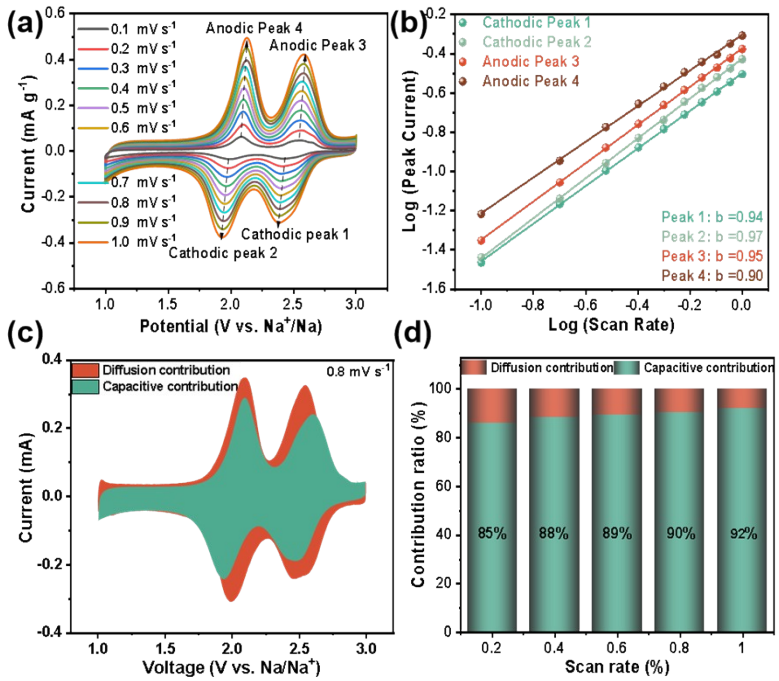

Figure S6. a) The CV curves of PBD-2 at different scan rates from 0.1 to 1.0 mV s^{-1}. b) Fitting lines of the b-values for PBD-2. c) The CV profile with capacitive and diffusion behaviors of PBD-2 at a scan rate of 0.8 mV s^{-1}. d) Capacitive contributions at different scan rates.

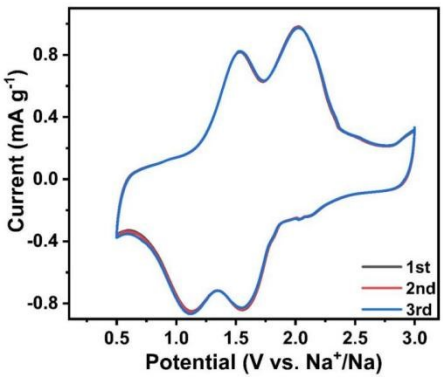

Figure S7. The CV curves of the PBD-1-based full cell at 2.0 mV s^{-1}.

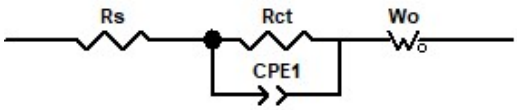

Figure S8. The equivalent circuits of EIS data for PBD in Na-ion batteries.

Table S1. The performances of PBD-1 electrodes were compared with the reported n-type cathodes in SIBs.

Materials	Cycling performance (capacity, current	Cycle number, capacity retention	Reference

	density, median voltage)	ratio	
PBQ	242.3 (mAh/g), 1 A/g 1.9 V	400, 91.3%	Energy Storage Materials, 2024, 70, 103561.[4]
PTCDI-DAQ @C	182 (mAh/g), 3 A/g 1.8 V	1000, 72.0%	Advanced Functional Materials, 2023, 33, 2300740.[5]
2PTCDI-4AQ	160 (mAh/g), 1 A/g 1.7 V	800, 96.0%	Acs Sustainable Chemistry & Engineering, 2024, 12, 4576-4586.[6]
HOFs-8	120 (mAh/g), 10C 2.2 V	5000, 85.3%	Advanced Functional Materials, 2024, 34, 2314851.[7]
PTAD	191.4 (mAh/g), 2 A/g 1.8 V	1500, 70.0%	Acs Nano, 2024, 18, 4159-4169.[8]
PPQ	90 (mAh/g), 800 mA/g 2.2 V	700, 93.3%	Chemical Engineering Journal, 2022, 449, 137745.[9]
$C_6Cl_4O_2$	150 (mAh/g), 10 mA/g 2.7 V	20, 20%	Chemistry of Materials, 2015, 27, 7258-7264.[10]
PBD-1	143 (mAh/g), 5C 2.3 V	2500, 91%	This work

Table S2. Elemental analysis of PBD-1.

Weight Ratio	**C (%)**	**H (%)**	**S (%)**
Experimental Value	**63.21**	**2.25**	**20.69**
Theoretical Value	**65.29**	**2.05**	**21.78**

References

1. Lu, T. and F. Chen, *Multiwfn: A multifunctional wavefunction analyzer.* Journal of Computational Chemistry, 2012. **33**(5): p. 580-592.
2. Grimme, S., S. Ehrlich, and L. Goerigk, *Effect of the Damping Function in Dispersion Corrected Density Functional Theory.* Journal of Computational Chemistry, 2011. **32**(7): p. 1456-1465.
3. Li, X., et al., *The transport properties of sodium-ion in the low potential platform region of oatmeal-derived hard carbon for sodium-ion batteries.* Journal of Alloys and Compounds, 2019. **787**: p. 229-238.
4. Zhang, W., et al., *Intermolecular interaction promoted polymer cathode for ultrahigh capacity*

utilization and ultrafast ion diffusion of sodium metal battery. Energy Storage Materials, 2024. **70**: p. 103561.

5. Yu, F., et al., *Organic-Carbon Core-Shell Structure Promotes Cathode Performance for Na-Ion Batteries.* Advanced Functional Materials, 2023. **33**(29): p. 2300740.
6. Hu, J., et al., *A Macromolecule Cathode for High-Performance Li-Ion and Na-Ion Batteries.* Acs Sustainable Chemistry & Engineering, 2024. **12**(11): p. 4576-4586.
7. Guo, C., et al., *Chemical-Stabilized Aldehyde-Tuned Hydrogen-Bonded Organic Frameworks for Long-Cycle and High-Rate Sodium-Ion Organic Batteries.* Advanced Functional Materials, 2024. **34**(21): p. 2314851.
8. Kim, E.Y., et al., *A Carbonyl and Azo-Based Polymer Cathode for Low-Temperature Na-Ion Batteries.* Acs Nano, 2024. **18**(5): p. 4159-4169.
9. Li, D., et al., *Phenanthraquinone-based polymer organic cathodes for highly efficient Na-ion batteries.* Chemical Engineering Journal, 2022. **449**: p. 137745.
10. Kim, H., et al., *High Energy Organic Cathode for Sodium Rechargeable Batteries.* Chemistry of Materials, 2015. **27**(21): p. 7258-7264.